European Journal of Medicinal Chemistry 85 (2014) 207–214

Contents lists available at ScienceDirect

European Journal of Medicinal Chemistry

journal homepage: http://www.elsevier.com/locate/ejmech

Original article

Novel metal complexes of naphthalimide–cyclam conjugates as potential multi-target receptor tyrosine kinase (RTK) inhibitors: Synthesis and biological evaluation

Shaoying Tan [a], Kun Han [b], Qiang Li [a], Linjiang Tong [b], Yiqi Yang [a], Zhuo Chen [a, *], Hua Xie [b, *], Jian Ding [b], Xuhong Qian [a], Yufang Xu [a, *]

[a] State Key Laboratory of Bioreactor Engineering, Shanghai Key Laboratory of Chemical Biology, Shanghai Key Laboratory of New Drug Design, School of Pharmacy, East China University of Science and Technology, Shanghai 200237, China
[b] Division of Anti-tumor Pharmacology, State Key Laboratory of Drug Research, Shanghai Institute of Materia Medica, Chinese Academy of Sciences, Shanghai 201203, China

ARTICLE INFO

Article history:
Received 19 March 2014
Received in revised form
2 July 2014
Accepted 20 July 2014
Available online 22 July 2014

Keywords:
Metal complexes
Naphthalimide
Cyclam
RTK inhibitors
Antiproliferation
Antiangiogenesis

ABSTRACT

A novel series of metal complexes of naphthalimide–cyclam conjugates were synthesized and their *in vitro* antitumor activities were evaluated. The newly-synthesized compounds showed huge diversity of antiproliferative potency due to variety of metal ions and length of alkyl chains, among which the Zn(II) and Cr(III) complexes exhibited comparable antiproliferative activities with amonafide via multiple tyrosine kinase inhibition. Further research revealed that the representative compound **8a** displayed broad-spectrum antiproliferative activity against 15 cancer cell lines with average IC_{50} value 10.18 ± 3.25 μM, and effective antiangiogenic activity on human microvascular endothelial cells (HMEC-1). In brief, metal complexes of naphthalimide–cyclam conjugates were firstly designed and synthesized as multi-target tyrosine kinase inhibitors and proved of their antitumor capacities.

1. Introduction

Receptor tyrosine kinases (RTKs) are a superfamily of transmembrane proteins which play critical roles in the transduction of extracellular signals to the cytoplasm. They are tightly regulated in normal cells. Aberrantly activated RTKs are implicated with tumor growth, progression and metastasis by modulating downstream signaling pathways [1–3]. Tyrosine kinase inhibitors are verified of their effective antitumor activities, and are approved in clinical use. And more of them able to target RTKs are in clinical trials. For example, Gefitinib (trade name Iressa) is an EGFR inhibitor approved for the treatment of patients with breast, lung and other cancers [4,5]. Nevertheless, single RTK inhibitors tempted to induce point mutations and drug resistance according to the clinical data which reveals that patients responded to targeted therapies initially when treated with specific tyrosine kinase inhibitors, but most of them relapsed later [6]. Moreover, redundant and adaptable molecular pathways between individual patients and within tumors in the same patients thwart the efficiency of treatment targeting a single RTK.

Tyrosine kinase inhibitors which modulate a limited number of tyrosine kinases are therapeutically more useful by overcoming drug resistance and crippling the alternative pathways of cancer cells [7,8]. Taking the multi-target RTK inhibitor sorafenib for example, it could simultaneously inhibit vascular endothelial growth factor receptor 2 (VEGFR-2), PDGFR-β, FMS-like tyrosine kinase 3 (Flt-3), Raf kinase and stem cell factor receptor (c-kit)) [9]. The success of dasatinib [6] (Bcr/Abl and Src) and sunitinib (VEGFR-1, -2, and-3, PDGFR-α, and -β, Flt-3 and colony stimulating factor 1 receptor (CSF-1R)) also supports the importance of multi-target RTK inhibitors [10,11].

Angiogenesis, or new blood vessel formation, is limited in healthy adults, but crucial in sustaining tumor growth and metastasis [12]. Therefore, developing angiogenesis inhibitors is a

Abbreviation: CSF-1R, colony stimulating factor 1 receptor; Cyclam, 1,4,8,11-tetraazamacrocycle; DDQ, 2,3-dichloro-5,6-dicyano-benzoquinone; Flt-3, FMS-like tyrosine kinase 3; HMEC, human microvascular endothelial cells; RTK, Receptor Tyrosine Kinase; VEGFR2, vascular endothelial growth factor receptor 2.

* Corresponding authors.
E-mail addresses: chenzhuo@ecust.edu.cn, chenzhuo@mail.ecust.edu.cn (Z. Chen), hxie@simm.ac.cn (H. Xie), yfxu@ecust.edu.cn (Y. Xu).

http://dx.doi.org/10.1016/j.ejmech.2014.07.068
0223-5234/

recommendable antitumor strategy as few side effects might be expected [13]. RTKs, or VEGFR, FGFR and PDGFR in detail, are involved as therapeutic targets which regulate the angiogenic process in growing tumors [14,15]. For example, the small-molecule tyrosine kinase inhibitors sunitinib and sorafinib exhibits clinical efficacy in patients with highly-vascularized renal cell cancer [16,17].

Cyclam (1,4,8,11-tetraazamacrocycle) is one of the most widely-used macrocyclic polyamines and attracts continuous attention due to its biological properties and its importance in coordination chemistry. Cyclam derivatives and their metal-ion complexes are applied in medical trials for diagnosis and the treatment of AIDs [18,19]. Medical interest of cyclam derivatives in the treatment of tumors is also emerging. For example, Silbert et al. developed two new lipophilic cyclam derivatives with IC_{50} values below 10 μM against cancer cell line L1210 and demonstrated that the introduction of lipophilic substitution could improve the ability of antiproliferative activity [20]. Paola and cooperators certificated that the positive antitumor activity could probably be ascribed to an increased lipophilicity of cyclam for the improvement of transportation across cell membrane [21]. On the other hand, cyclam can complex various transition metal ions with high kinetic and thermodynamic stability because of its strong affinity [22] which was disadvantageous for selective metal chelating, but benefit for medical application. It is reported that cyclam could chelate with Zn(II) and Cu(II) to inhibit cancer cells growth [23–25].

Previously, we reported our work on developing naphthalimide derivatives as angiogenesis-related RTK inhibitors [26]. Naphthalimide derivatives were widespread of its antitumor potency, but were seldom studied of their RTK inhibition activity before [27–29]. Herein, naphthalimide–cyclam conjugates were designed to improve their antitumor capacities and further functionalized with various lipophilic alkyls and complexed with Zn(II), Cu(II), Ni(II), Co(II), Cr(III). We demonstrated that these novel compounds, especially Zn(II) and Cr(III) complexes, were proved to possess comparable antiproliferative activities with amonafide due to multi-target RTK inhibition activities. The representative compound **8a** exhibited dual effects in vitro antiproliferation and antiangiogenesis.

2. Results and discussions

2.1. Chemistry

Compounds **4a**–**4d** were synthesized in four steps from 4-bromo-naphathalimide as shown in Scheme 1. Firstly, 4-bromo-naphathalimide was refluxed in ethanol with corresponding primary amino to obtain **1a**–**1d**. Compounds **1a**–**1d** were reacted with ethanol amine under Ullmann's condition to get **2a**–**2d**, which further were converted to **3a**–**3d** in the existence of 2,3-dichloro-5,6-dicyano-benzoquinone (DDQ), tetrabutyl ammonium bromide and triphenylphosphine. Then compounds **4a**–**4d** were obtained from cyclam condensed with **3a**–**3d** in $CHCl_3$ (see Scheme 2).

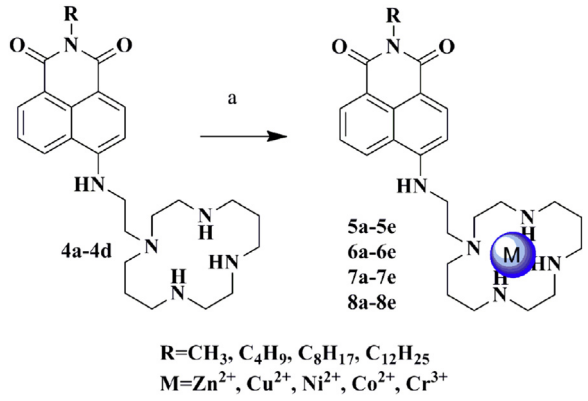

Scheme 2. Synthesis of target metal complexes. (a) Corresponding metal salt, CH_3OH, r.t., 6 h.

The metal complexes (**5a**–**5e**, **6a**–**6e**, **7a**–**7e** and **8a**–**8e**) were obtained with a mild, high-yield one-step method by compounds **4a**–**4d** condensed with $Zn(ClO_4)_2$, $Ni(ClO_4)_2$, $Cu(ClO_4)_2$, $Co(ClO_4)_2$, and $Cr(ClO_4)_3$ in methanol, respectively.

2.2. In vitro cytotoxic activity of metal complexes

Firstly, the antiproliferative activity of naphthlimide–cyclam conjugates **4a**–**4d** and their metal complexes **5a**–**5e**, **6a**–**6e**, **7a**–**7e** and **8a**–**8e** were evaluated against human breast carcinoma cell lines MDA-MB-231 and MDA-MB-435, human ducal breast epithelial tumor cell line T47D and human breast epithelial cell line HBL-100. As shown in Table 1, the antiproliferative activities of the target compounds were affected by the length of alkyl chains and variety of metal ions. Normally speaking, the derivatives with long alkyl chains inhibited growth of cancer cells more significantly than their short alkyl chain analogues, such as **4d** v.s. **4b** and **8a** v.s. **6a**, against the tested cell lines. The results were in accordance with our previous work [26,30]. Meanwhile, the introduction of different metal ions led to the diversity of the antiproliferative activity. Zn(II), Cr(III)-cyclam complexes generally reduced cell proliferation better than the derivatives of other metal ions and exhibited comparable activity with amonafide. Taking **8a**–**8e** for example, the IC_{50} value of **8a** and **8d** against MDA-MB-231 were at single-digital micromolar range, while other metal complexes were 2–8 folds less potent than **8a** and **8d**. Most of the metal complexes showed better cytotoxic activities against MDA-MB-231 and MDA-MB-435 than T47D. As for the normal human breast cell line HBL-100, the tested

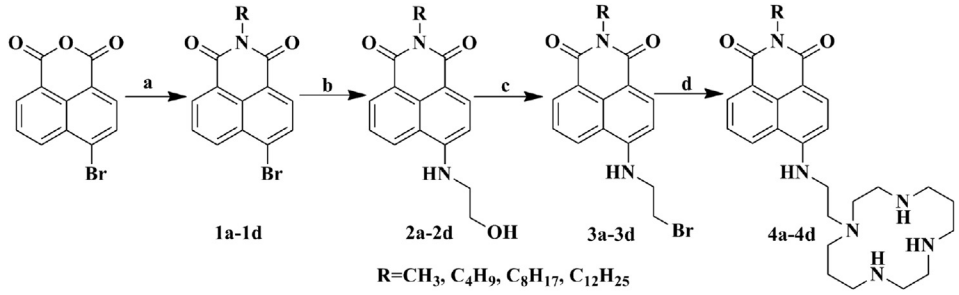

Scheme 1. Synthesis of target compounds **4a**–**4d**. (a) Corresponding primary amines, ethanol, reflux, 3 h; (b) ethanol amine, methoxyethanol, reflux, 4 h (c) DDQ, PPh_3, $(n\text{-butyl})_4NBr$, CH_2Cl_2, r.t., 12 h; (d) cyclam, KI, $CHCl_3$, reflux, 6 h.

Table 1
Antiproliferative activity of parent compounds and cyclam fused naphthalimides metal complexes.

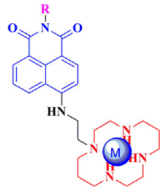

compound	$R=$	$M=$	Antiproliferative activity (IC_{50}, μM)			
			MDA-MB-231	MDA-MB-435	T47D	HBL-100
4a	CH_3	/	12.66	17.89	39.43	N.D.[a]
5a	CH_3	$Zn(ClO_4)_2$	14.47	23.97	90.93	>50
5b	CH_3	$Cu(ClO_4)_2$	>100	>100	>100	N.D.
5c	CH_3	$Ni(ClO_4)_2$	34.94	35.67	92.04	N.D.
5d	CH_3	$Cr(ClO_4)_3$	9.53	10.04	26.02	>50
5e	CH_3	$Co(ClO_4)_2$	41.17	43.37	86.79	N.D.
4b	C_4H_9	/	23.09	23.04	36.23	N.D.
6a	C_4H_9	$Zn(ClO_4)_2$	19.24	33.16	41.36	>50
6b	C_4H_9	$Cu(ClO_4)_2$	>100	>100	>100	N.D.
6c	C_4H_9	$Ni(ClO_4)_2$	30.26	35.16	34.81	N.D.
6d	C_4H_9	$Cr(ClO_4)_3$	10.79	14.60	22.33	>50
6e	C_4H_9	$Co(ClO_4)_2$	38.89	49.39	36.23	N.D.
4c	C_8H_{17}	/	8.78	8.50	25.08	N.D.
7a	C_8H_{17}	$Zn(ClO_4)_2$	8.08	22.56	22.64	>50
7b	C_8H_{17}	$Cu(ClO_4)_2$	51.19	40.11	21.96	N.D.
7c	C_8H_{17}	$Ni(ClO_4)_2$	35.43	56.18	57.03	N.D.
7d	C_8H_{17}	$Cr(ClO_4)_3$	6.50	9.09	7.33	31.58
7e	C_8H_{17}	$Co(ClO_4)_2$	39.06	78.08	35.27	N.D.
4d	$C_{12}H_{25}$	/	6.73	10.32	19.88	N.D.
8a	$C_{12}H_{25}$	$Zn(ClO_4)_2$	8.00	22.33	19.32	>50
8b	$C_{12}H_{25}$	$Cu(ClO_4)_2$	63.42	72.44	17.56	N.D.
8c	$C_{12}H_{25}$	$Ni(ClO_4)_2$	10.72	18.87	>100	N.D.
8d	$C_{12}H_{25}$	$Cr(ClO_4)_3$	6.53	9.23	30.41	>50
8e	$C_{12}H_{25}$	$Co(ClO_4)_2$	53.42	69.56	68.63	N.D.
Amonafide			5.10	5.36	19.07	N.D.

[a] N.D. : not determined.

compounds (**5a**, **5d**, **6a**, **6d**, **7a**, **7d**, **8a** and **8d**), exhibited 1–7 folds less potent cytotoxic activities against normal cell line in contrast to cancer cell lines. The results revealed that these compounds exhibited certain selective against tumor cell lines.

2.3. Receptor tyrosine kinase (RTK) inhibitory activity

Furthermore, representative compounds **8a** and **8d** and their precursor **4d** were evaluated of their RTK inhibition activities by ELISA experiment. According to Table 2, the naphthalimide–cyclam conjuagate **4d** could inhibit 4 of the tested 14 RTKs, namely ErbB4, c-Src, Abl, c-Met. Its Cr^{3+} complex **8d** exhibited wider and stronger RTK inhibition activities against 5 of the tested 14 RTKs, which were ErbB4, c-Src, Abl, c-Met and IGF1R. What's more, the Zn^{2+} complex **8a** could effectively inhibit not only RTK which would be concerned with tumor proliferation and so on, like Flt-1, EGFR, ErbB4, c-Src, Abl, c-Met, and IGF1R, but also angiogenesis-related RTKs, including VEGFR2 and FGFR1 [31,32].

Table 2
Inhibitory activity of **4d**, **8a** and **8d** to tyrosine kinases.

Tyrosine kinase	IC_{50} (μM) ± SD		
	4d	**8a**	**8d**
Flt-1	>10.0	4.07 ± 1.56	>10.0
VEGFR-2	>10.0	6.00 ± 1.15	>10.0
PDGFR-α	>10.0	>10.0	>10.0
PDGFR-β	>10.0	>10.0	>10.0
RET	>10.0	>10.0	>10.0
EGFR	>10.0	3.35 ± 1.21	>10.0
ErbB2	>10.0	>10.0	>10.0
ErbB4	0.92 ± 0.72	0.80 ± 0.59	0.61 ± 0.12
c-Src	0.47 ± 0.11	0.42 ± 0.05	0.87 ± 0.32
ABL	7.44 ± 1.23	0.32 ± 0.10	0.52 ± 0.08
EPH-A2	>10.0	>10.0	>10.0
c-Met	0.42 ± 0.21	0.21 ± 0.14	0.07 ± 0.03
IGF1R	>10.0	1.75 ± 0.49	0.61 ± 0.23
FGFR1	>10.0	2.68 ± 0.73	>10.0

2.4. Antiproliferative activity of *8a*

As demonstrated above, **8a** exhibited broad-spectrum RTK inhibition activities as expected and potent antitumor activity to the tested three human breast cancer cell lines. We further evaluated compound **8a** as potential antitumor drug. Firstly, we studied the antiproliferative activity of **8a** against fifteen human cancer cell lines from various tissues in vitro, including one human promyelocytic leukemia cell line (HL 60), two human hepatocellular carcinoma cell lines (SMMC-7H, BEL-7402), two human lung adenocarcinoma cell lines (SGC-7901, A549), two human breast adenocarcinoma cell lines (MDA-MB-468, MDA-MB-231, MCF-7), one human cervical carcinoma cell line (Hela), one human pancreatic carcinoma cell line (BXPC-3), one human ovarian carcinoma cell line (SKOV3), one human colon carcinoma cell line (HCT-116), one human caucasian prostate adenocarcinoma cell line (PC-3), one human nasopharyngeal carcinoma cell line (KB), one human epidermoid carcinoma cell line (A431) and one human kidney carcinoma cell line (786-O). As shown in Fig. 1, **8a** could inhibit the growth of most of the cancer cells potently, with IC_{50} values ranging from 4.86 to 15.30 μM, and 10.18 ± 3.25 μM on average. For example, the IC_{50} values were 4.86 ± 1.50 μM against BEL-7402 and 5.47 ± 0.65 μM against MDA-MB-468. Meanwhile, the antiproliferative activities against 786-O and SMMC-7721 were relatively poor (the IC_{50} value 15.30 ± 2.63 μM and 14.13 ± 0.84 μM, respectively). The result indicated that **8a** was a potential broad-spectrum antiproliferative agent.

2.5. Anti-angiogenesis activity of *8a*

2.5.1. Inhibition of migration and tube formation

According to the results of RTK inhibition activities, the representative metal ion complex **8a** could simultaneously inhibit VEGFR2, PDGFRα and β, and FGFR, which were involved in the process of angiogenesis. To investigate whether **8a** could inhibit the migration of HMEC-1 cells (human microvascular endothelial cell line), transwell Boyden chamber assay was performed. As illustrated in Fig. 2a, about 44% of the migrated HMEC-1 cells were inhibited in the present of 5 μM **8a**, which indicated that **8a** could effectively inhibit the migration of cancer cells. Further research

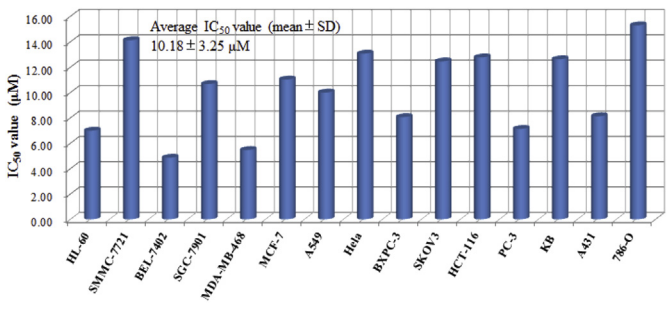

Fig. 1. Antitumor effect of **8a** in 15 cancer cell lines.

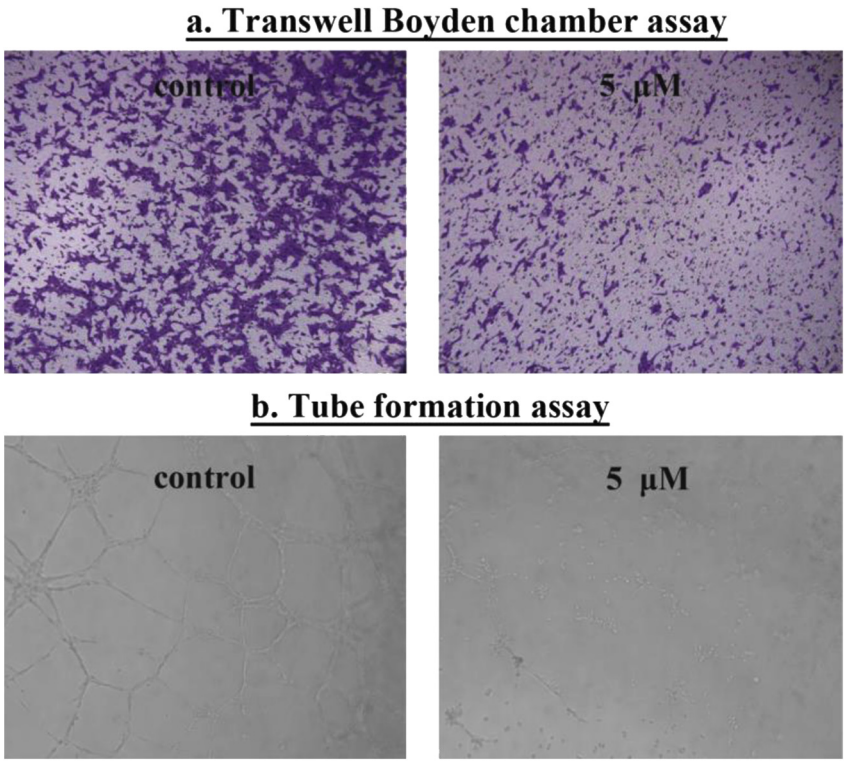

Fig. 2. Inhibitory effect of **8a** on HMEC-1 cells migration and tube formation activities. a) Representative images showing inhibition of migration, b) Representative images showing inhibition of tube formation.

about the inhibitory effect to the formation of functional tubes was performed in the HMEC-1 cells. The results revealed that the functional tubes were nearly completely destroyed when exposed in 5 μM **8a**.

*2.5.2. Down-regulation of downstream signaling pathways by **8a***

Furthermore, we evaluated the effect of **8a** on the key downstream signaling pathways of RTK by western blotting, including AKT and Erk. As shown in Fig. 3, compound **8a** caused little change at the concentration of 1.25 μM and 2.5 μM. It induced dose-dependent decrease in phosphorylation of AKT in HMEC-1 cells at the concentration of 5 μM and 10 μM. In detail, phosphor-AKT and Erk declined after exposure to 5 μM **8a** and became undetectable at exposure to 10 μM **8a**.

3. Conclusion

In all, to develop novel multi-target RTK inhibitors, a series of metal complexes of naphthalimide–cyclam conjugates were designed and synthesized. The newly-synthesized compounds exhibited structure–activity relationship due to the diversity of length of alkyl chains and complexes of metal ions. Among the target compounds, derivatives with long alkyl chains and their Zn(II), Cr(III)-complexes exhibited effective antiproliferative effect. Furthermore, **8a**, as representative compound, was evaluated as a potential multi-target RTK inhibitor. It was certified to be a broad-spectrum antiproliferative agent against 15 cancer cell lines with an average IC_{50} value at 10.18 ± 3.25 μM. It was also proved of effective antiangiogenic activity on human microvascular endothelial cells (HMEC-1). Further research certified that **8a** could down-regulate downstream signaling pathway of RTKs. In summary, novel metal complexes of napthalimide–cyclam conjugates were verified of their potential antitumor capacities from both antiproliferative and antiangiogenic activities as multi-target RTK inhibitors.

4. Experimental section

All the chemical regents and solvents were analytic grade. All the synthesized fused naphthalimide–cyclam conjugates were confirmed by ^{1}H NMR, ^{13}C NMR and HRMS, while the metal complexes were verified by HRMS and HPLC except the Cr(III) complexes. ^{1}H NMR and ^{13}C NMR were measured on a Bruker AV-400

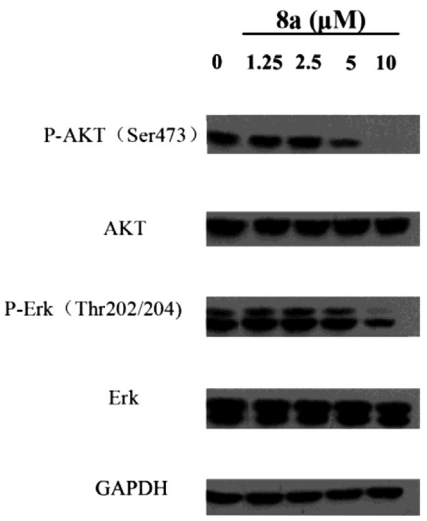

Fig. 3. Induction of the down-regulated Erk1/2 (Thr 202/204) and AKT (Ser 473) signaling pathways induced in HMEC-1 cells in the present of **8a**.

spectrometer (in $CDCl_3$ and DMSO-d_6, TMS as an internal standard). HRMS were collected in the Center of Analysis & Test of East China University of Science and Technology. Analytical HPLC was performed on a Hewlett–Packard 1100 system chromatograph equipped with photodiode array detector. SRB was purchased from Sigma Aldrich (St. Louis, MO, USA); all medium and FBS from Gibco (Grand Island, NY, USA); Matrigel from BD Biosciences (San Jose, CA, USA); antibodies to extracellular signal-regulated kinase (Erk) and AKT from Cell Signaling Technology (Danvers, MA, USA); antibody to GAPDH (glyceraldehyde-3-phosphate dehydrogenase) from KangChen Bio-tech (Shanghai); secondary antibodies from Calbiochem (San Diego, CA, USA).

4.1. Synthesis

4.1.1. General procedure for the preparation of **1a**–**1d**

6-bromobenzo[de]-isochromene-1,3-dione (1.94 g, 7.00 mmol) was dissolved in 20 ml ethanol. Then corresponding primary amine (7.70 mmol) was added, and the mixture was stirred at 60 °C for 5–6 h. The mixture was cooled to room temperature and evaporated in vacuum to obtain the residue. Then the residue was purified on silica gel chromatography (PE: EA = 10:1, V/V) to provide **1a**–**1d**.

*4.1.1.1. 6-Bromo-2-methyl-1H-benzo[de]isoquinoline-1,3(2H)-dione (**1a**).* White solid, yield: 90%. ^{1}H NMR (400 MHz, $CDCl_3$): δ 8.68 (d, J = 7.2 Hz, 1H), 8.59 (d, J = 8.4 Hz, 1H), 8.44 (d, J = 8.0 Hz, 1H), 8.06 (d, J = 7.6 Hz, 1H), 7.86 (t, J = 8.4 Hz, 1H), 3.57 (s, 3H); MS(ESI) calcd for $C_{13}H_9BrNO_2$ $[M+H]^+$ 289.0, found: 289.0.

*4.1.1.2. 6-Bromo-2-butyl-1H-benzo[de]isoquinoline-1,3(2H)-dione (**1b**).* White solid, yield: 80%. ^{1}H NMR (400 MHz, $CDCl_3$) δ 8.66 (d, J = 7.2 Hz, 1H), 8.56 (d, J = 8.8 Hz, 1H), 8.41 (d, J = 8.0 Hz, 1H), 8.04 (d, J = 8.0 Hz, 1H), 7.85 (t, J = 8.0 Hz, 1H), 4.19 (t, J = 7.6 Hz, 1H), 1.77–1.69 (m, 2H), 1.51–1.42 (m, 2H), 1.00 (t, J = 7.2 Hz, 3H); MS(ESI) calcd for $C_{16}H_{15}BrNO_2$ $[M+H]^+$ 331.0, found: 331.0.

*4.1.1.3. 6-Bromo-2-octyl-1H-benzo[de]isoquinoline-1,3(2H)-dione (**1c**).* White solid, yield: 85%. ^{1}H NMR (400 MHz, $CDCl_3$): δ 8.68 (d, J = 7.2 Hz, 1H), 8.59 (d, J = 7.6 Hz, 1H), 8.44 (d, J = 8.0 Hz, 1H), 8.06 (d, J = 8.0 Hz, 1H), 7.87 (t, J = 7.6 Hz, 1H), 4.18 (t, J = 8.0 Hz, 2H), 1.78–1.71 (m, 2H), 1.47–1.29 (m, 10H), 0.89 (t, J = 7.2 Hz, 3H); MS(ESI) calcd for $C_{20}H_{23}BrNO_2$ $[M+H]^+$ 387.1, found: 387.1.

*4.1.1.4. 6-Bromo-2-dodecyl-1H-benzo[de]isoquinoline-1,3(2H)-dione (**1d**).* White solid, yield: 85%. ^{1}H NMR (400 MHz, $CDCl_3$): δ 8.68 (d, J = 7.2 Hz, 1H), 8.59 (d, J = 8.4 Hz, 1H), 8.44 (d, J = 7.6 Hz, 1H), 8.06 (d, J = 8.0 Hz, 1H), 7.87 (t, J = 7.6 Hz, 1H), 4.18 (t, J = 7.6 Hz, 2H), 1.78–1.71 (m, 2H), 1.47–1.27 (m, 18H), 0.90 (t, J = 7.2 Hz, 3H); MS(ESI) calcd for $C_{24}H_{31}BrNO_2$ $[M+H]^+$ 443.1, found: 443.2.

4.1.2. General procedure for the preparation of **2a**–**2d**

1a–**1d** (6 mmol) were dissolved in 50 ml 2-methoxyethanol, respectively. Then ethanol amine (24 mmol) was added and the mixture was refluxed for 6 h. 150 ml water was added and solid was precipitated immediately. The crude production was obtained by suction filtration and was purified on silica gel chromatography (CH_2Cl_2: MeOH = 50:1–20:1, V/V).

*4.1.2.1. 6-(2-Hydroxyethylamino)-2-methyl-1H-benzo[de]isoquinoline-1,3(2H)-dione (**2a**).* Yellow solid, yield: 90%. ^{1}H NMR (400 MHz, CD_3COCD_3): δ 8.59 (d, J = 8.4 Hz, 1H), 8.50 (d, J = 7.6 Hz, 1H), 8.37 (d, J = 8.4 Hz, 1H), 7.68 (t, J = 8.0 Hz, 1H), 6.89 (d, J = 8.4 Hz, 1H), 3.92 (t, J = 5.6, 2H), 3.62 (t, J = 5.6, 2H), 3.42 (s, 3H); MS(ESI) calcd for $C_{15}H_{15}N_2O_3$ $[M+H]^+$ 270.1, found: 270.1.

*4.1.2.2. 6-(2-Hydroxyethylamino)-2-butyl-1H-benzo[de]isoquinoline-1,3(2H)-dione (**2b**).* Yellow solid, yield: 87%. ^{1}H NMR (400 MHz, $CDCl_3$): δ 8.58 (d, J = 7.2 Hz, 1H), 8.46 (d, J = 8.4 Hz, 1H), 8.16 (d, J = 8.4 Hz, 1H), 7.64 (t, J = 8.4 Hz, 1H), 6.79 (d, J = 8.4 Hz, 1H), 4.17 (t, J = 7.6 Hz, 2H), 4.09 (t, J = 5.2 Hz, 2H), 3.60 (t, J = 5.2 Hz, 1H), 1.74–1.70 (m, 2H), 1.49–1.43 (m, 2H), 0.99 (t, J = 7.6 Hz, 3H). MS(ESI) calcd for $C_{18}H_{21}N_2O_3$ $[M+H]^+$ 312.1, found: 312.1.

*4.1.2.3. 6-(2-Hydroxyethylamino)-2-octyl-1H-benzo[de]isoquinoline-1,3(2H)-dione (**2c**).* Yellow solid, yield: 84%. ^{1}H NMR (400 MHz, $CDCl_3$): δ 8.57 (d, J = 7.2 Hz, 1H), 8.45 (d, J = 8.4 Hz, 1H), 8.13 (d, J = 8.4 Hz, 1H), 7.62 (t, J = 7.6 Hz, 1H), 6.74 (d, J = 8.4 Hz, 1H), 4.16 (t, J = 8.0 Hz, 2H), 4.09 (t, J = 5.2 Hz, 2H), 3.60 (t, J = 5.2 Hz, 2H), 1.77–1.70 (m, 2H), 1.47–1.28 (m, 10H), 0.89 (t, J = 7.2 Hz, 3H); MS(ESI) calcd for $C_{22}H_{29}N_2O_3$ $[M+H]^+$ 369.2, found: 369.2.

*4.1.2.4. 6-(2-Hydroxyethylamino)-2-dodecyl-1H-benzo[de]isoquinoline-1,3(2H)-dione (**2d**).* Yellow solid, yield: 84%. ^{1}H NMR (400 MHz, $CDCl_3$): δ 8.53 (d, J = 7.2 Hz, 1H), 8.41 (d, J = 8.4 Hz, 1H), 8.11 (d, J = 8.0 Hz, 1H), 7.59 (t, J = 8.0 Hz, 1H), 6.71 (d, J = 8.4 Hz, 1H), 4.15 (t, J = 7.6 Hz, 2H), 4.09 (t, J = 5.2 Hz, 2H), 3.58 (t, J = 5.2 Hz, 2H), 1.76–1.69 (m, 2H), 1.45–1.26 (m, 18H), 0.89 (t, J = 7.2 Hz, 3H); MS(ESI) calcd for $C_{26}H_{37}N_2O_3$ $[M+H]^+$ 425.3, found: 425.3.

4.1.3. General procedure for the preparation of **3a**–**3d**

2,3-dichloro-5,6-dicyano-1,4-benzoquinone (0.41 g, 1.80 mmol) and Triphenyl Phosphine (0.47 g, 1.80 mmol) were dissolved in 10 ml dry $CHCl_3$. Then the mixture of tetrabutyl ammonium bromide (0.58 g, 1.80 mmol), **2a**–**2d** (1.50 mmol, respectively) and 10 ml dry $CHCl_3$ was dropped. 6 h later, the solvent was concentrated by vacuum and **3a**–**3d** were purified on silica gel chromatography (CH_2Cl_2).

*4.1.3.1. 6-((2-Bromoethyl)amino)-2-methy-1H-benzo[de]isoquinoline-1,3(2H)-dione (**3a**).* Orange solid, yield: 75%. ^{1}H NMR (500 MHz, $CDCl_3$): δ 8.63 (d, J = 7.3 Hz, 1H), 8.50 (d, J = 7.2 Hz, 1H), 8.15 (d, J = 8.3 Hz, 1H), 7.69 (t, J = 8.0 Hz, 1H), 6.75 (d, J = 6.9 Hz, 1H), 3.89 (t, J = 5.8 Hz, 2H), 3.76 (t, J = 5.7 Hz, 2H), 3.54 (s, 3H); MS(ESI) calcd for $C_{15}H_{14}BrN_2O_2$ $[M+H]^+$ 332.0, found: 332.0.

*4.1.3.2. 6-((2-Bromoethyl)amino)-2-butyl-1H-benzo[de]isoquinoline-1,3(2H)-dione (**3b**).* Orange solid, yield: 68%. ^{1}H NMR (400 MHz, $CDCl_3$): δ 8.62 (d, J = 7.2 Hz, 1H), 8.49 (d, J = 8.4 Hz, 1H), 8.15 (d, J = 8.4 Hz, 1H), 7.68 (t, J = 7.6 Hz, 1H), 6.76 (d, J = 8.4 Hz, 1H), 4.18 (t, J = 7.6 Hz, 2H), 3.89 (t, J = 6.0 Hz, 2H), 3.77 (t, J = 6.0 Hz, 1H), 1.77–1.69 (m, 2H), 1.51–1.41 (m, 2H), 0.99 (t, J = 7.2 Hz, 3H). MS (ESI) calcd for $C_{18}H_{20}BrN_2O_2$ $[M+H]^+$ 375.1, found: 375.0.

*4.1.3.3. 6-((2-Bromoethyl)amino)-2-octyl-1H-benzo[de]isoquinoline-1,3(2H)-dione (**3c**).* Orange solid, yield: 85%. ^{1}H NMR (400 MHz, $CDCl_3$): δ 8.63 (d, J = 6.4 Hz, 1H), 8.50 (d, J = 8.4 Hz, 1H), 8.16 (d, J = 7.6 Hz, 1H), 7.69 (t, J = 8.0 Hz, 1H), 6.77 (d, J = 8.4 Hz, 1H), 5.60 (br, 1H), 4.17 (t, J = 7.6 Hz, 2H), 3.89 (q, J = 4.4 Hz, 2H), 3.77 (t, J = 6.0 Hz, 2H), 1.78–1.70 (m, 2H), 1.47–1.28 (m, 10H), 0.89 (t, J = 7.2 Hz, 3H); MS(ESI) calcd for $C_{22}H_{28}BrN_2O_2$ $[M+H]^+$ 431.1, found: 431.1.

*4.1.3.4. 6-((2-Bromoethyl)amino)-2-dodecyl-1H-benzo[de]isoquinoline-1,3(2H)-dione (**3d**).* Orange solid, yield: 83%. ^{1}H NMR (400 MHz, $CDCl_3$): δ 8.63 (d, J = 7.2 Hz, 1H), 8.50 (d, J = 8.4 Hz, 1H), 8.16 (d, J = 8.0 Hz, 1H), 7.69 (t, J = 8.4 Hz, 1H), 6.77 (d, J = 8.4 Hz, 1H), 5.60 (br, 1H), 4.17 (t, J = 7.6 Hz, 2H), 3.89 (t, J = 5.6 Hz, 2H), 3.77 (t, J = 6.0 Hz, 2H), 1.78–1.70 (m, 2H), 1.45–1.27 (m, 18H), 0.90 (t, J = 7.2 Hz, 3H), MS(ESI) calcd for $C_{26}H_{36}$ BrN_2O_2 $[M+H]^+$ 487.2, found: 487.2.

*4.1.4. General procedure for the preparation of **4a–4d***

1,4,8,11-Tetraazacyclotetradecane (0.10 g, 0.50 mmol) was dissolved in 10 ml dry $CHCl_3$. Then the mixture of **3a–3d** (0.20 mmol, respectively) and 15 ml dry $CHCl_3$ was dropped in r.t. under the argon. 3 days later, the solvent was concentrated by vacuum and **4a–4d** was purified on silica gel chromatography (CH_2Cl_2:MeOH:Ammonium Hydroxide = 100:15:2).

*4.1.4.1. 6-((2-(1,4,8,11-Tetraazacyclotetradecan-1-yl)ethyl)amino)-2-methyl-1H-benzo [de]isoquinoline-1,3(2H)-dione (**4a**).* Orange solid, yield: 50%. ^{1}H NMR (400 MHz, CD_3OD): δ 8.24–8.18 (m, 2H), 8.05 (d, J = 8.4 Hz, 1H), 7.40 (t, J = 8.4 Hz, 1H), 6.59 (d, J = 8.4 Hz, 1H), 3.50 (t, J = 7.2, 2H), 3.34 (s, 3H), 2.78–2.53 (m, 18H), 1.79–1.71 (m, 4H); ^{13}C NMR (100 MHz, CD_3OD): δ 164.90, 164.37, 150.86, 134.32, 130.67, 129.58, 127.81, 123.98, 121.81, 120.38, 107.94, 103.68, 54.35, 53.48, 50.74, 50.47, 49.15, 48.34, 46.69, 40.19, 27.40, 25.33, 24.05; HRMS (ESI) calcd for $C_{25}H_{37}N_6O_2$ $[M+H]^+$ 453.2978, found: 453.2968.

*4.1.4.2. 6-((2-(1,4,8,11-Tetraazacyclotetradecan-1-yl)ethyl)amino)-2-butyl-1H-benzo [de]isoquinoline-1,3(2H)-dione (**4b**).* Orange solid, yield: 66%. ^{1}H NMR (400 MHz, $CDCl_3$): δ 9.09 (d, J = 8.0 Hz, 1H), 8.58 (d, J = 6.8 Hz, 1H), 8.43 (d, J = 8.4 Hz, 1H), 7.80 (t, J = 6.0 Hz, 1H), 7.66 (t, J = 7.6 Hz, 1H), 6.68 (d, J = 8.8 Hz, 1H), 4.17 (t, J = 7.6 Hz, 2H), 3.79 (d, J = 5.6 Hz, 2H), 3.09–3.03 (m, 4H), 2.97 (br, 2H), 2.89 (br, 2H), 2.73 (t, J = 4.8 Hz, 2H), 1.77–1.69 (m, 2H), 1.49–1.43 (m, 2H), 0.98 (t, J = 7.2 Hz, 3H). ^{13}C NMR (100 MHz, $CDCl_3$): δ 164.8, 164.2, 150.4, 134.5, 131.3, 130.1, 128.9, 124.4, 122.8, 120.7, 109.2, 103.5, 51.2, 51.0, 50.8, 50.6, 47.2, 46.8, 46.4, 46.0, 45.1, 40.1, 40.0, 30.3, 25.8, 25.2, 20.5, 13.9; HRMS (ESI) calcd for $C_{28}H_{43}N_6O_2$ $[M+H]^+$ 495.3448, found: 495.3454.

*4.1.4.3. 6-((2-(1,4,8,11-Tetraazacyclotetradecan-1-yl)ethyl)amino)-2-octyl-1H-benzo [de]isoquinoline-1,3(2H)-dione (**4c**).* Orange solid, yield: 65%. ^{1}H NMR (400 MHz, CD_3OD): δ 8.31–8.28 (m, 2H), 8.16 (d, J = 8.4 Hz, 1H), 7.45 (t, J = 8.0 Hz, 1H), 6.66 (d, J = 8.8 Hz, 1H), 3.99 (t, J = 7.2 Hz, 2H), 3.50 (t, J = 6.4 Hz, 2H), 2.77–2.51 (m, 18H), 1.77–1.62 (m, 6H), 1.31–1.23 (m, 10H), 0.85 (t, J = 7.2 Hz, 3H); ^{13}C NMR (100 MHz, CD_3OD): δ 164.39, 163.81, 150.74, 134.30, 130.56, 129.56, 127.73, 123.87, 121.88, 120.25, 108.07, 103.62, 54.53, 53.67, 50.78, 50.60, 49.31, 48.51, 46.76, 40.25, 39.68, 31.64, 29.14, 29.05, 27.88, 27.56, 26.94, 25.40, 22.36, 13.20; HRMS (ESI) calcd for $C_{32}H_{51}N_6O_2$ $[M+H]^+$ 551.4074, found: 551.4070.

*4.1.4.4. 6-((2-(1,4,8,11-Tetraazacyclotetradecan-1-yl)ethyl)amino)-2-dodecyl-1H-benzo[de]isoquinoline-1,3(2H)-dione (**4d**).* Orange solid, yield: 62%. ^{1}H NMR (400 MHz, CD_3OD): δ 8.33–8.29 (m, 2H), 8.18 (d, J = 8.4 Hz, 1H), 7.47 (t, J = 8.0 Hz, 1H), 6.67 (d, J = 8.8 Hz, 1H), 4.00 (t, J = 7.2 Hz, 2H), 3.52 (t, J = 6.4 Hz, 2H), 2.78–2.53 (m, 18H), 1.77–1.63 (m, 6H), 1.31–1.19 (m, 18H), 0.85 (t, J = 7.2 Hz, 3H); ^{13}C NMR (100 MHz, CD_3OD): δ 164.40, 163.83, 150.74, 134.33, 130.58, 129.60, 127.77, 123.89, 121.92, 120.28, 108.12, 103.62, 54.49, 53.69, 50.81, 50.61, 49.31, 48.51, 46.75, 40.28, 39.70, 31.73, 29.44, 29.21, 29.15, 27.92, 27.51, 26.95, 25.40, 22.41, 13.25; HRMS (ESI) calcd for $C_{36}H_{59}N_6O_2$ $[M+H]^+$ 607.4700, found: 607.4688.

*4.1.5. General procedure for the preparation of **5a–5e**, **6a–6e**, **7a–7e** and **8a–8e***

4a–4d (0.05 mmol) were dissolved in 2 ml CH_3OH, respectively, then six different salts in CH_3OH were added, respectively. 10 min to 2 h later, the solid was precipitated. The crude production was obtained by suction filtration and was washed twice with CH_3OH to get purity **5a–5e**, **6a–6e**, **7a–7e** and **8a–8e**.

*4.1.5.1. 6-((2-(1,4,8,11-Tetraazacyclotetradecan-1-yl)ethyl)amino)-2-methyl-1H-benzo [de]isoquinoline-1,3(2H)-dione-Zn(II)$(ClO_4)_2$ (**5a**).* HRMS (ESI) calcd for $C_{25}H_{35}N_6O_2Zn$ $[M]^+$ 515.2107, found: 515.2094.

*4.1.5.2. 6-((2-(1,4,8,11-Tetraazacyclotetradecan-1-yl)ethyl)amino)-2-methyl-1H-benzo [de]isoquinoline-1,3(2H)-dione-Cu(II)$(ClO_4)_2$ (**5b**).* HRMS (ESI) calcd for $C_{25}H_{35}N_6O_2Cu$ $[M]^+$ 514.2112, found: 514.2114.

*4.1.5.3. 6-((2-(1,4,8,11-Tetraazacyclotetradecan-1-yl)ethyl)amino)-2-methyl-1H-benzo [de]isoquinoline-1,3(2H)-dione-Ni(II)$(ClO_4)_2$ (**5c**).* HRMS (ESI) calcd for $C_{25}H_{35}N_6O_2Ni$ $[M]^+$ 509.2169, found: 509.2154.

*4.1.5.4. 6-((2-(1,4,8,11-Tetraazacyclotetradecan-1-yl)ethyl)amino)-2-methyl-1H-benzo [de]isoquinoline-1,3(2H)-dione-Co(II)$(ClO_4)_2$ (**5e**).* HRMS (ESI) calcd for $C_{25}H_{34}N_6O_2Co$ $[M]^+$ 509.2070, found: 509.2061.

*4.1.5.5. 6-((2-(1,4,8,11-Tetraazacyclotetradecan-1-yl)ethyl)amino)-2-butyl-1H-benzo [de]isoquinoline-1,3(2H)-dione-Zn(II)$(ClO_4)_2$ (**6a**).* HRMS (ESI) calcd for $C_{28}H_{41}N_6O_2Zn$ $[M]^+$ 557.2577, found: 557.2557.

*4.1.5.6. 6-((2-(1,4,8,11-Tetraazacyclotetradecan-1-yl)ethyl)amino)-2-butyl-1H-benzo [de]isoquinoline-1,3(2H)-dione-Cu(II)$(ClO_4)_2$ (**6b**).* HRMS (ESI) calcd for $C_{28}H_{41}N_6O_2Cu$ $[M]^+$ 556.2582, found: 556.2579.

*4.1.5.7. 6-((2-(1,4,8,11-Tetraazacyclotetradecan-1-yl)ethyl)amino)-2-butyl-1H-benzo [de]isoquinoline-1,3(2H)-dione-Ni(II)$(ClO_4)_2$ (**6c**).* HRMS (ESI) calcd for $C_{28}H_{41}N_6O_2Ni$ $[M]^+$ 551.2639, found: 551.2618.

*4.1.5.8. 6-((2-(1,4,8,11-Tetraazacyclotetradecan-1-yl)ethyl)amino)-2-butyl-1H-benzo[de]isoquinoline-1,3(2H)-dione-Co(II)$(ClO_4)_2$ (**6e**).* HRMS (ESI) calcd for $C_{28}H_{40}N_6O_2Co$ $[M]^+$ 551.2545, found: 551.2544.

*4.1.5.9. 6-((2-(1,4,8,11-Tetraazacyclotetradecan-1-yl)ethyl)amino)-2-octyl-1H-benzo [de]isoquinoline-1,3(2H)-dione-Zn(II)$(ClO_4)_2$ (**7a**).* HRMS (ESI) calcd for $C_{32}H_{49}N_6O_2Zn$ $[M]^+$ 613.3203, found: 613.3208.

*4.1.5.10. 6-((2-(1,4,8,11-Tetraazacyclotetradecan-1-yl)ethyl)amino)-2-octyl-1H-benzo [de]isoquinoline-1,3(2H)-dione-Cu(II)$(ClO_4)_2$ (**7b**).* HRMS (ESI) calcd for $C_{32}H_{49}N_6O_2Cu$ $[M]^+$ 607.3265, found: 607.3248.

*4.1.5.11. 6-((2-(1,4,8,11-Tetraazacyclotetradecan-1-yl)ethyl)amino)-2-octyl-1H-benzo [de]isoquinoline-1,3(2H)-dione-Ni(II)$(ClO_4)_2$ (**7c**).* HRMS (ESI) calcd for $C_{32}H_{49}N_6O_2Ni$ $[M]^+$ 612.3208, found: 612.3205.

*4.1.5.12. 6-((2-(1,4,8,11-Tetraazacyclotetradecan-1-yl)ethyl)amino)-2-octyl-1H-benzo[de]isoquinoline-1,3(2H)-dione-Co(II)$(ClO_4)_2$ (**7e**).* HRMS (ESI) calcd for $C_{32}H_{48}N_6O_2Co$ $[M]^+$ 607.3165, found: 607.3150.

*4.1.5.13. 6-((2-(1,4,8,11-Tetraazacyclotetradecan-1-yl)ethyl)amino)-2-dodecyl-1H-benzo[de]isoquinoline-1,3(2H)-dione-Zn(II)$(ClO_4)_2$ (**8a**).* HRMS (ESI) calcd for $C_{36}H_{57}N_6O_2Co$ $[M]^+$ 669.3829, found: 669.3809.

*4.1.5.14. 6-((2-(1,4,8,11-Tetraazacyclotetradecan-1-yl)ethyl)amino)-2-dodecyl-1H-benzo[de]isoquinoline-1,3(2H)-dione-Cu(II)$(ClO_4)_2$ (**8b**).* HRMS (ESI) calcd for $C_{36}H_{57}N_6O_2Cu$ $[M]^+$ 668.3834, found: 668.3820.

*4.1.5.15. 6-((2-(1,4,8,11-Tetraazacyclotetradecan-1-yl)ethyl)amino)-2-dodecyl-1H-benzo[de]isoquinoline-1,3(2H)-dione-Ni(II)(ClO_4)$_2$ (**8c**).* HRMS (ESI) calcd for $C_{36}H_{57}N_6O_2Ni$ $[M]^+$ 663.3891, found: 663.3881.

*4.1.5.16. 6-((2-(1,4,8,11-Tetraazacyclotetradecan-1-yl)ethyl)amino)-2-dodecyl-1H-benzo[de]isoquinoline-1,3(2H)-dione-Co(II)(ClO_4)$_2$ (**8e**).* HRMS (ESI) calcd for $C_{36}H_{56}N_6O_2Co$ $[M]^+$ 663.3791, found: 663.3774.

4.2. Cell lines and cell culture

MDA-MB-231, MDA-MB-435, T47D, MDA-MB-468, MCF-7, A549, HeLa, BXPC-3, SKOV3, HCT-116, PC-3, KB, A431, 786-O and HMEC-1 were purchased from American Type Culture Collection (ATCC, Manassas, VA, USA). SMMC-7721, BEL-7402 and HL60 were obtained from the Institute of Biochemistry and Cell Biology, Chinese Academy of Sciences (Shanghai, China). SGC-7901 was obtained from Renji Hospital (Shanghai, China). They were maintained in strict accordance with the supplier's instructions and established procedures.

4.3. In vitro cytotoxicity assays of the **4a**–**4d**, **5a**–**5e**, **6a**–**6e**, **7a**–**7e** and **8a**–**8e**

MTT or SRB assay was applied to evaluate the in vitro cytotoxicity of target compounds. Cancer cells were plated and incubated for 24 h in 96-well plates. The cells were then treated with increasing concentration of compounds **4a**–**4d**, **5a**–**5e**, **6a**–**6e**, **7a**–**7e**, **8a**–**8e** and amonafide for a further 72 h. For HL60 cell line, 20 μL (5 mg/mL in 0.9% brine) of MTT (Sigma) was added to each well. The cells were then incubated for an additional 4 h, after which 100 μL of "triplex solution" (10% SDS-5% isobutanol-HCl, 12 mM) was added, and the cells were incubated overnight at 37 °C. The plates were read at 570 nm on the scanning multiwell spectrophotometer (MAX190™). The inhibition rate on cell proliferation was calculated as: inhibition rate = $(1 - A_{570\ \text{treated}}/A_{570\ \text{control}}) \times 100\%$. The IC_{50} values were obtained by the Logit method. Each experiment was repeated in triplicate. For the rest cell lines, cells were then fixed with 10% trichloroacetic acid and stained with sulforhodamine B (Sigma). Sulforhodamine B in the cells was dissolved in 10 mM Tris–HCl and was measured at 515 nm using a multiwell spectrophotometer (MAX190™, Molecular Devices, Sunnyvale, USA). The inhibition rate on cell proliferation was calculated as follows: inhibition rate = $(1 - A_{515\ \text{treated}}/A_{515\ \text{control}}) \times 100\%$. IC_{50} values were determined from the results of at least three independent tests and calculated from the inhibition curves.

4.4. Protein kinase assays

[33] Tyrosine kinase activity was determined by an enzyme-linked-immunosorbent assay (ELISA). Fifty microliters of 10 μmol/L ATP solution diluted in reaction buffer [50 mmol/L HEPES, pH 7.4, 20 mmol/L $MgCl_2$, 0.1 mmol/L Na_3VO_4, and 1 mmol/L DTT] was added to each well of 96-well plates pre-coated with 2.5 μg/well poly $(Glu, Tyr)_{4:1}$ (Sigma) as a substrate and then added increasing concentrations of tyrosine kinase. After incubation for 1 h at 37 °C, the plate was washed three times with phosphate buffered saline containing 0.1% Tween20 (PBST). After adding 100 μL of anti-phosphotyrosine (PY99; 1:1000 dilution) antibody, another 0.5 h incubation at 37 °C, the plate was washed three times and goat anti-mouse IgG horseradish peroxidase (100 μL of a 1:2000 dilution) diluted in PBST containing 5 mg/mL BSA was added. The plate was reincubated at 37 °C for 0.5 h and washed as before. Finally, 100 μL of color development solution (0.03% H_2O_2 and 2 mg/mL *o*-phenylenediamine in 0.1 mol/L citrate buffer, pH 5.4) was added and the plate was incubated at room temperature until color emerged. The reaction was terminated by the addition of 50 μL of 2 mol/L H_2SO_4, and then the plate was read using a multi-well spectrophotometer (MAX190™) at 490 nm. The inhibition rate (%) was calculated using the following equation: inhibition rate = $[1 - (A_{490\ \text{treated}}/A_{490\text{control}})] \times 100\%$.

4.5. Cell migration assay

[34] HMEC-1s migration was determined in a transwell Boyden chamber (Costar, MA, USA). Firstly, cell suspension (5×10^5 cells/mL) with different concentrations of **8a** or control was added to the upper compartment of the chamber. Secondly, 20% FBS MCDB131 medium and the same concentrations of **8a** or control were added to the lower compartment. After incubation 6 h at 37 °C, the inhibition of migration was calculated: inhibition of migration = $[1 - (A_{\text{compound}} - A_{\text{blank}})/(A_{\text{control}} - A_{\text{blank}})] \times 100\%$.

4.6. Tube formation assay

[35] Matrigel (75 μL $well^{-1}$) was used to coat 96-well plates and solidify after 8 h incubation at 37 °C. For investigation of neovessel disruption, HMEC-1s (1×10^5 cells/mL) were seeded on Matrigel and left to align for 24 h. The formed capillary-like structures or cords were exposed to **8a**, and then examined with an inverted phase contrast microscope (DP70, Olympus, Japan). The number of the tubes was quantified from five random fields. The inhibition of tube formation was calculated: inhibition of tube formation = $[1 - (\text{tubes}_{\text{compound}}/\text{tubes}_{\text{control}})] \times 100\%$.

4.7. Western blot analysis

HMEC-1s cells were plated into 6-well plate (3×10^5 cells/well) and incubated for 24 h. The cells were then exposed to corresponding compounds for 12 h for analysis of Erk and AKT signal transduction pathways. Whole-cell lysates were collected and boiled for 10 min in 2 × SDS sample buffer, subjected to 10% SDS-PAGE, and transferred to nitrocellulose (Amersham Life Sciences). The blot was blocked in blocking buffer (5% non-fat dry milk/1% Tween-20 in TBS) for 1 h at room temperature, and then incubated with primary antibodies (anti-phospho-AKT (1:500), anti-AKT (1:5000), anti-phospho-Erk (1:2000), anti-Erk (1:2000) and anti-GAPDH (1:10,000)) in blocking buffer for 2 h at room temperature. The bands were then visualized using horseradish peroxidase-conjugated secondary antibodies (1:2000) followed by ECL (Pierce Biotech, Rockford, IL).

Acknowledgment

This work is financially supported by the National Basic Research Program of China (973 Program, 2010CB126100), the National High Technology Research and Development Program of China (863 Program, 2011AA10A207), the National Natural Science Foundation of China (grants 21236002 and grants 21302054), the National Science & Technology Pillar Program, the Shanghai Committee of Science and Technology (Grant 13ZR1453100) and the Fundamental Research Funds for the Central Universities.

Appendix A. Supplementary data

Supplementary data related to this article can be found at http://dx.doi.org/10.1016/j.ejmech.2014.07.068.

References

[1] M.T. Conconi, G. Marzaro, L. Urbani, I. Zanusso, R. Di Liddo, I. Castagliuolo, P. Brun, F. Tonus, A. Ferrarese, A. Guiotto, A. Chilin, Quinazoline-based multi-tyrosine kinase inhibitors: synthesis, modeling, antitumor and antiangiogenic properties, Eur. J. Med. Chem. 67 (2013) 373–383.

[2] A. Arora, E.M. Scholar, Role of tyrosine kinase inhibitors in cancer therapy, J. Pharmacol. Exp. Ther. 315 (3) (2005) 971–979.

[3] A. Gschwind, O.M. Fischer, A. Ullrich, The discovery of receptor tyrosine kinases: targets for cancer therapy, Nat. Rev. Cancer 4 (5) (2004) 361–370.

[4] A.E. Wakeling, S.P. Guy, J.R. Woodburn, S.E. Ashton, B.J. Curry, A.J. Barker, K.H. Gibson, ZD1839 (Iressa): an orally active inhibitor of epidermal growth factor signaling with potential for cancer therapy, Cancer Res. 62 (20) (2002) 5749–5754.

[5] J. Yang, L.J. Wang, J.J. Liu, L. Zhong, R.L. Zheng, Y. Xu, P. Ji, C.H. Zhang, W.J. Wang, X.D. Lin, L.L. Li, Y.Q. Wei, S.Y. Yang, Structural optimization and structure–activity relationships of N2-(4-(4-Methylpiperazin-1-yl)phenyl)-N8-phenyl-9H-purine-2,8-diamine derivatives, a new class of reversible kinase inhibitors targeting both EGFR-activating and resistance mutations, J. Med. Chem. 55 (23) (2012) 10685–10699.

[6] M. Talpaz, N.P. Shah, H. Kantarjian, N. Donato, J. Nicoll, R. Paquette, J. Cortes, S. O'Brien, C. Nicaise, E. Bleickardt, M.A. Blackwood-Chirchir, V. Iyer, T.T. Chen, F. Huang, A.P. Decillis, C.L. Sawyers, Dasatinib in imatinib-resistant philadelphia chromosome-positive leukemias, N. Engl. J. Med. 354 (24) (2006) 2531–2541.

[7] A. Gangjee, N. Zaware, S. Raghavan, M. Ihnat, S. Shenoy, R.L. Kisliuk, Single agents with designed combination chemotherapy potential: synthesis and evaluation of substituted Pyrimido[4,5-b]indoles as receptor tyrosine kinase and thymidylate synthase inhibitors and as antitumor agents, J. Med. Chem. 53 (4) (2010) 1563–1578.

[8] S. Faivre, S. Djelloul, E. Raymond, New paradigms in anticancer therapy: targeting multiple signaling pathways with kinase inhibitors, Semin. Oncol. 33 (4) (2006) 407–420.

[9] S.M. Wilhelm, L. Adnane, P. Newell, A. Villanueva, J.M. Llovet, M. Lynch, Preclinical overview of sorafenib, a multikinase inhibitor that targets both Raf and VEGF and PDGF receptor tyrosine kinase signaling, Mol. Cancer Ther. 7 (10) (2008) 3129–3140.

[10] A.M. O'Farrell, T.J. Abrams, H.A. Yuen, T.J. Ngai, S.G. Louie, K.W.H. Yee, L.M. Wong, W. Hong, L.B. Lee, A. Town, B.D. Smolich, W.C. Manning, L.J. Murray, M.C. Heinrich, J.M. Cherrington, SU11248 is a novel FLT3 tyrosine kinase inhibitor with potent activity in vitro and in vivo, Blood 101 (9) (2003) 3597–3605.

[11] D.B. Mendel, A.D. Laird, X. Xin, S.G. Louie, J.G. Christensen, G. Li, R.E. Schreck, T.J. Abrams, T.J. Ngai, L.B. Lee, L.J. Murray, J. Carver, E. Chan, K.G. Moss, J.O. Haznedar, J. Sukbuntherng, R.A. Blake, L. Sun, C. Tang, T. Miller, S. Shirazian, G. McMahon, J.M. Cherrington, In vivo antitumor activity of SU11248, a novel tyrosine kinase inhibitor targeting vascular endothelial growth factor and platelet-derived growth factor receptors: determination of a pharmacokinetic/pharmacodynamic relationship, Clin. Cancer Res. 9 (1) (2003) 327–337.

[12] J. Zhang, Y. Zhang, Y. Shan, N. Li, W. Ma, L. He, Synthesis and preliminary biological evaluation of novel taspine derivatives as anticancer agents, Eur. J. Med. Chem. 45 (7) (2010) 2798–2805.

[13] K.M. Cook, W.D. Figg, Angiogenesis inhibitors: current strategies and future prospects, CA: Cancer J. Clin. 60 (4) (2010) 222–243.

[14] K. Gotink, H.W. Verheul, Anti-angiogenic tyrosine kinase inhibitors: what is their mechanism of action? Angiogenesis 13 (1) (2010) 1–14.

[15] N. Ferrara, R.S. Kerbel, Angiogenesis as a therapeutic target, Nature 438 (7070) (2005) 967–974.

[16] R.J. Motzer, R.M. Bukowski, Targeted therapy for metastatic renal cell carcinoma, J. Clin. Oncol. 24 (35) (2006) 5601–5608.

[17] B. Escudier, T. Eisen, W.M. Stadler, C. Szczylik, S. Oudard, M. Siebels, S. Negrier, C. Chevreau, E. Solska, A.A. Desai, F. Rolland, T. Demkow, T.E. Hutson, M. Gore, S. Freeman, B. Schwartz, M. Shan, R. Simantov, R.M. Bukowski, Sorafenib in advanced clear-cell renal-cell carcinoma, N. Engl. J. Med. 356 (2) (2007) 125–134.

[18] X. Liang, P.J. Sadler, Cyclam complexes and their applications in medicine, Chem. Soc. Rev. 33 (4) (2004) 246.

[19] F. Liang, S. Wan, Z. Li, X. Xiong, L. Yang, X. Zhou, C. Wu, Medical applications of macrocyclic polyamines, Curr. Med. Chem. 13 (6) (2006) 711–727.

[20] J.W. Sibert, A.H. Cory, J.G. Cory, Lipophilic derivatives of cyclam as new inhibitors of tumor cell growth, Chem. Commun. 0 (2) (2002) 154–155.

[21] C. Saudan, P. Ceroni, V. Vicinelli, V. Balzani, M. Gorka, S.K. Lee, F. Vögtle, M. Orlandi, G. Bartolini, S. Tavolari, P. Rocchi, A.M. Ferreri, Simple and dendritic cyclam derivatives. Photophysical properties, effect of protonation and Zn^{2+} coordination, preliminary screening as inhibitors of tumour cell growth, Supramol. Chem. 16 (8) (2004) 541–548.

[22] D.K. Cabbiness, D.W. Margerum, Macrocyclic effect on the stability of copper(II) tetramine complexes, J. Am. Chem. Soc. 91 (23) (1969) 6540–6541.

[23] K.L. Haas, K.J. Franz, Application of metal coordination chemistry to explore and manipulate cell biology, Chem. Rev. 109 (10) (2009) 4921–4960.

[24] A.R. Lam, S. Bhattacharya, K. Patel, S.E. Hall, A. Mao, N. Vaidehi, Importance of receptor flexibility in binding of cyclam compounds to the chemokine receptor CXCR4, J. Chem. Information Model. 51 (1) (2010) 139–147.

[25] J.C. Joyner, J. Reichfield, J.A. Cowan, Factors influencing the DNA nuclease activity of iron, cobalt, nickel, and copper chelates, J. Am. Chem. Soc. 133 (39) (2011) 15613–15626.

[26] X. Wang, Z. Chen, L. Tong, S. Tan, W. Zhou, T. Peng, K. Han, J. Ding, H. Xie, Y. Xu, Naphthalimides exhibit in vitro antiproliferative and antiangiogenic activities by inhibiting both topoisomerase II (topo II) and receptor tyrosine kinases (RTKs), Eur. J. Med. Chem. 65 (0) (2013) 477–486.

[27] M.F. Brana, A. Ramos, Naphthalimides as anti-cancer agents: synthesis and biological activity, Curr. Med. Chem. Anticancer Agents 1 (3) (2001) 237–255.

[28] X.L. Li, Y.J. Lin, Q.Q. Wang, Y.K. Yuan, H. Zhang, X.H. Qian, The novel anti-tumor agents of 4-triazol-1,8-naphthalimides: synthesis, cytotoxicity, DNA intercalation and photocleavage, Eur. J. Med. Chem. 46 (4) (2011) 1274–1279.

[29] I. Ott, X. Qian, Y. Xu, D.H.W. Vlecken, I.J. Marques, D. Kubutat, J. Will, W.S. Sheldrick, P. Jesse, A. Prokop, C.P. Bagowski, A gold(I) phosphine complex containing a naphthalimide ligand functions as a TrxR inhibiting antiproliferative agent and angiogenesis inhibitor, J. Med. Chem. 52 (3) (2009) 763–770.

[30] Z. Chen, X. Liang, H.Y. Zhang, H. Xie, J.W. Liu, Y.F. Xu, W.P. Zhu, Y. Wang, X. Wang, S.Y. Tan, D. Kuang, X.H. Qian, A new class of naphthalimide-based antitumor agents that inhibit topoisomerase II and induce lysosomal membrane permeabilization and apoptosis, J. Med. Chem. 53 (6) (2010) 2589–2600.

[31] E. Zwick, J. Bange, A. Ullrich, Receptor tyrosine kinase signalling as a target for cancer intervention strategies, Endocrine-related Cancer 8 (3) (2001) 161–173.

[32] D.R. Robinson, Y.M. Wu, S.F. Liu, The protein tyrosine kinase family of the human genome, Oncogene 19 (49) (2000) 5548–5557.

[33] L.J. Tong, H. Xie, T. Peng, X.F. Liu, X.L. Xin, X. Huang, S.M. Chen, H.Y. Liu, H.L. Li, M.Y. Geng, M. Yin, J. Ding, Establishment of platform for screening insulin-like growth factor-1 receptor inhibitors and evaluation of novel inhibitors, Acta Pharmacol. Sin. 32 (7) (2011) 930–938.

[34] K. Osusky, D. Hallahan, A. Fu, F. Ye, Y. Shyr, L. Geng, The receptor tyrosine kinase inhibitor SU11248 impedes endothelial cell migration, tubule formation, and blood vessel formation in vivo, but has little effect on existing tumor vessels, Angiogenesis 7 (3) (2004) 225–233.

[35] A. Kruczynski, M. Poli, R. Dossi, E. Chazottes, G. Berrichon, C. Ricome, R. Giavazzi, B.T. Hill, G. Taraboletti, Anti-angiogenic, vascular-disrupting and anti-metastatic activities of vinflunine, the latest vinca alkaloid in clinical development, Eur. J. Cancer 42 (16) (2006) 2821–2832.